
AVF inversion of Anelastic Reflectivity: Practical issues concerning implementation.

Chris Bird, Kristopher Innanen, Larry Lines, Mostafa Naghizadeh

ABSTRACT

A frequency by frequency method (AVF) of inverting for Q exists which requires as input an estimate of the local spectrum of the absorptive reflection coefficient. We have a calibrated fast S-transform (FST) which we have demonstrated provides a high fidelity estimate of the local spectra of seismic reflection events and is suitable as input for AVF inversion. In this paper we consider a prioritized set of issues a method like this face when applied in the field. We develop methodologies and recommendations to manage: 1. Random/uncorrelated noise; 2. Nearby/difficult-to-isolate events; 3. Source wavelet. We begin by describing our synthetic testing environment including forward model for attenuating traces, and then consider each of these ideas in turn. In their presence we consider AVF inversion, though more complicated, to be a likely tractable problem. An SEG abstract by Wu et al. indicates that other research groups are making encouraging though not fully confirmed progress in this regard.

INTRODUCTION

Absorption is the progressive decay of the highest frequencies of a seismic pulse as it travels through Earth material (O'Doherty and Anstey, 1971). The effect is that the peak amplitude decays and the pulse becomes broader (O'Doherty and Anstey, 1971). The quality factor, Q , is a measure of how absorptive an Earth material is, a low Q value corresponds to a highly absorptive material. The ability to determine Q presents an important problem in exploration seismology because absorption is closely related to rock fluid properties such as viscosity, porosity and fluid saturation (Quan and Harris, 1997; Vasheghani and Lines, 2009). Absorption is not easy to measure in the field as it is difficult to isolate the effect of absorption on the seismic pulse from other attenuation mechanisms (Sheriff and Geldart, 1995) such as geometrical spreading and scattering. However, methods of determining Q exist including the centroid frequency method which uses the shift in average frequency between two points to determine Q (Quan and Harris, 1997).

A less well known influence of Q on reflection data is in the reflection coefficients which attend a strong Q contrast (Lines et al., 2008; Innanen, 2011); a growing body of field (Odebeatu et al., 2006; Bird and Innanen, 2011b) and lab (Lines et al.) evidence suggests such dispersive reflectivity may indeed be present in hydrocarbon relevant geophysical regimes.

A frequency by frequency method (AVF) of inverting for Q developed by Innanen (2011) exists which requires as input an estimate of the local spectrum of the absorptive reflection coefficient. We have a calibrated fast S-transform (FST) which we have demonstrated provides a high fidelity estimate of the local spectra of seismic reflection events (Bird et al., 2010b) and is suitable as input for AVF inversion. In this paper we consider a prioritized set of issues a method like this face when applied in the field. We de-

velop methodologies and recommendations to manage: 1. Random/uncorrelated noise; 2. Nearby/difficult-to-isolate events; 3. Source wavelet. We begin by describing our synthetic testing environment including forward model for attenuating traces, and then consider each of these ideas in turn. In their presence we consider AVF inversion, though more complicated, to be a likely tractable problem. An SEG abstract by Wu et al. indicates that other research groups are making encouraging though not fully confirmed progress in this regard.

PROXIMAL REFLECTIONS

In order to implement AVF inversion to estimate Q of a target, we need an estimate of the local spectrum of the target reflection coefficient. However, the low frequency spectrum of the reflection will be interfered with by nearby seismic events such as proximal independent reflections, multiples, etc. The more proximal two events are the greater the portion of their spectra will interfere. Hence, the spectrum of a target reflection will be contaminated by the spectra of neighboring reflection events, the portion of the spectrum which will be interfered with is a function of how proximal the other event is. An event which is far away will only interfere with the target at very low frequencies but closer events will interfere at higher frequencies. It is unavoidable that, in the presence of nearby events, the only high fidelity estimate of the target reflection's spectrum we can obtain is at the high frequencies.

SYNTHETIC DATA

We begin by modeling a synthetic seismogram which contains a single absorptive reflection coefficient which is preceded in time by a large number of reflection events. We start with an Earth model consisting of an elastic overburden overlaying a highly absorptive target ($Q=13$). Figure 1 is a diagram of the simple Earth model used to generate the synthetic absorptive reflections. The absorptive reflection is generated for an impulsive plane wave normally incident on the target. Then this single absorptive reflection is added to a synthetic trace with a large number of elastic reflections which precede the absorptive reflection in time, with the number of samples between the absorptive reflection and the nearest elastic spike reflection being a controlled variable. We define the number of samples between the target absorptive reflection and the nearest elastic reflection event as the separation distance. Figure 1(a) shows an example trace, the isolated reflection near 3.7 seconds is the absorptive reflection, it can clearly be seen that the separation distance is quite large for this trace. The traces were then input into the FST and the local spectrum of the absorptive reflection coefficient was obtained. The extracted spectrum of the absorptive reflection was then used to invert for Q of the target media (Bird et al., 2010a). The numerical experiment is repeated with the separation distance reduced. Figure 1(a) shows an example trace in which the separation distance is quite large and Figure 1(b) shows the local spectrum of the absorptive reflection in blue extracted using the FST and what the spectrum of the absorptive reflection would be without any other events present in red. Figure 2 is similar to Figure 1 except that the separation distance has been reduced. In Figure 1 we see that the separation is quite large but in Figure 2 the event separation is narrowed significantly. The effect of the decrease in the separation distance of events results in a greater portion of the local spectrum of the absorptive reflection was interfered with by the spectra of the nearby events. This is apparent when we compare Figure 1(b) to Figure 2(b), notice that in Figure 2(b), where the separation distance is quite small, there is a greater portion

of the spectrum of the absorptive reflection coefficient which is interfered with. However, we see in Figure 2 that the estimate of the spectrum in the presence of numerous events (red) tracks the analytic spectrum (blue) at the high frequency range. Therefore, by only using the high frequencies we may implement AVF inversion (Innanen, 2011; Bird et al., 2010a). In Figure 3 I have plotted the inverted value of Q in red, the actual value of Q used to model the reflection ($Q=13$) against the separation distance. We can see that the AVF inversion estimate of Q is quite reliable until a separation distance of 1 sample is reached and then the estimate blows up.

Further, to gain more statistical significance of the inversion results, I have run this same experiment described above but I have allowed Q to range from 8 to 46. Figure 4 shows the result of this experiment. There are 9 panels in Figure 4, for each panel the separation distance is fixed and the separation distance decreases from panel 1 to panel 9. Then in each panel Q of the target reflector is varied from 8 to 46 and the inversion is compared to the actual Q value used in the modeling. As can clearly be seen, there is an inconsistent ability of the AVF inversions ability to predict Q . For instance, in panel 4(e) the separation distance is 209 samples but the inversion is entirely inaccurate for nearly all values of Q . Then in panel 4(f), where the separation distance is 154 samples (and hence, the inversion result should be even less accurate) we see that the inversion is exceptional at predicting Q . This surprising result would suggest that the nature of the event nearest the absorptive reflection has a greater impact on the inversion result than the separation distance. The inconsistency of the AVF inversion, as a function of separation distance, needs to be explored further.

RANDOM NOISE

Because random noise is present in any seismic experiment, it is necessary to test the effectiveness of AVF inversion in the presence of noise if we hope to ever implement it on real seismic data. In order to perform this testing, synthetic seismic traces were generated with a single absorptive reflection coefficient. Then 3% percent random noise was added and the traces were input into the FST and an estimate of the absorptive reflections spectrum was extracted and used to invert for Q . Figure 6 shows 9 attempts at performing AVF inversion on noisy traces. In each panel, the actual Q value (black) and the inverted Q value (red) are shown. The experiment was repeated 9 times. Notice that the result of the inversion is extremely poor. This is not surprising as the FST algorithm averages over short time windows at high frequencies, for example see Naghizadeh and Innanen (2010) and so noise will have a significant contribution to the output of the FST at high frequencies. To combat the effect of noise, repeat experiments could be performed (i.e. acquire numerous traces) and then the traces stacked to attenuate the random noise. To model this, we generated a large number of these synthetic traces with noise and stacked them. This stacking does an excellent job of attenuating the random noise. Figure 7 and Figure 8 show examples of how stacking improves the fidelity of the FST estimate of the spectrum of the reflection coefficient. In Figure 7, ten repeat traces are stacked together and it is seen that the inversion has improved somewhat. In Figure 8 however, 35 traces have been stacked and the inversion has improved even more. Notice from Figure 7 and Figure 8 that the inversion works best when Q is low. This is also expected as the variability of the reflection coefficient is higher for a larger contrast in Q .

WAVELET AND DECONVOLUTION

In order to implement AVF inversion to estimate Q of a target, we need an estimate of the local spectrum of the targets reflection coefficient. However, the embedded wavelet imposes a footprint onto the spectrum of the reflection which needs to be removed in order to implement AVF inversion. To remove the effect of the embedded wavelet we can perform deconvolution of the seismic trace. To test how effective AVF inversion may be on deconvolved traces a number of synthetic traces were generated with a single absorptive reflection convolved with a minimum phase wavelet. We use the simple Earth model, as shown in Figure 1 used to generate the synthetic absorptive reflections, consisting of an elastic overburden overlaying a highly attenuative target. The traces generated from this model were then deconvolved using the weiner deconvolution codes from the CREWES toolbox. Next the deconvolved trace was input into the FST to obtain an estimate of the absorptive reflection coefficient. This spectrum was then used to invert for Q using the modified AVF framework (Bird et al., 2010a; Innanen, 2011). Figure 10 shows an example of a deconvolved trace using the CREWES toolbox deconvolution codes. Figure 10(a) shows an absorptive reflection coefficient, in Figure 10(b) there is the absorptive reflection coefficient convolved with a minimum phase wavelet, in Figure 10(c) we see the result of deconvolution. The resulting deconvolved traces, such as that shown in Figure 10(c) were input into the FST and a spectrum of the reflection was extracted, an example of this is shown in Figure 11. The blue curve in Figure 11 is the FST spectrum of the absorptive reflection, the red curve in Figure 11 is the FST spectrum of the reflection after deconvolution. Notice that the amplitudes of the deconvolved result are lower than the spectrum of analytic reflection, this is because the deconvolution code performs an rms power balancing of the input trace and the output deconvolved trace. This may be due to the fact that the deconvolved result is broader band than the input trace and hence there is a discrepancy between the amplitudes of the deconvolved result and the analytic amplitude spectrum. We can see this in the time domain, Figure 12(a) shows a random reflectivity series, Figure 12(b) shows that reflectivity series convolved with a wavelet and Figure 12(c) shows the deconvolution result. Notice that the amplitudes of the reflections in the deconvolved result are less than the amplitudes of the original reflectivity series. This discrepancy needs to be fixed before AVF inversion can be implemented accurately. A solution was found by plotting the amplitude spectra of input traces with an embedded wavelet and the output deconvolved result. Figure 13 shows an example this, the blue curve is the spectrum of a trace with random reflectivity convolved with a wavelet, we see the effect of the wavelet is to give "shape" to the spectrum which is controlled by the dominant frequencies of the wavelet. As can clearly be seen, The dominant frequencies lie roughly between 10 and 35 Hz. The deconvolved result is shown in black, it has the spectrum of a white reflectivity. The rms power balancing performed by the deconvolution codes uses the entire spectrum to balance the input trace and the deconvolved result and therefore since the input trace has a sharp drop of in amplitude after 30 Hz, the mean amplitudes of the deconvolved result is somewhere between the high amplitude portion of the input trace (ie. between 10 - 35 Hz) and the very low amplitudes at all other frequencies. As we can see in Figure 13 this is true, the amplitudes of the deconvolved result are less than the high amplitude portion of the input trace but higher than the input trace everywhere else, this is why the spectrum of the deconvolved result shown in red in Figure 11 are less than the analytic amplitudes. Therefore in order to fix this, a ratio of the mean amplitudes of the deconvolved result and

the input trace were found for the dominant frequency range of the input trace and then this ratio was used to boost the amplitudes of the deconvolved result. Figure 14 is the same as Figure 13 except that it highlights the region for which the ratio of mean amplitudes was extracted with vertical red lines. After applying the correction, the amplitude spectrum of the corrected deconvolved result and the analytic reflection are shown in Figure 15, notice that the spectra of the corrected deconvolved result is much closer to the spectrum of the analytic reflection.

INVERSION RESULTS

With the correction to the amplitude spectrum of deconvolved traces, through an interpretive step, applied it is possible to use the corrected spectrum to invert for Q (Innanen, 2011; Bird et al., 2010a). The individual effects of noise, proximal events and a seismic wavelet have been examined for their effect on the local spectrum of a absorptive reflection. To test AVF inversion, synthetic traces were generated which included all of these effects with a target absorptive reflection embedded near the centre of the synthetic trace containing noise, numerous reflection events, and a wavelet. An example of one of these traces is shown in Figure 16 which highlights the absorptive reflection event. These traces are generated using a random reflectivity and zeroing out a specified number of samples in the middle of the trace to control the separation distance and inserting an absorptive reflection. These traces are then convolved with a wavelet and random noise. AVF inversion can be implemented by first stacking a number of these traces to attenuate the effect of random noise. Then deconvolving the traces and performing the mean amplitude matching as described in the previous section is performed to remove the effect deconvolving the wavelet. Finally, the traces were input into the FST and the spectrum of the reflection was obtained. The high frequency portion only was suitable for AVF inversion due to the contamination of the low frequencies by proximal events. Figure 17 shows an example of a spectrum of the absorptive reflection coefficient extracted using the FST from the trace shown in Figure 15. It can be seen from Figure 17 that deconvolution and then mean amplitude matching yields an estimate of the spectrum of the absorptive reflection which seems reasonable. However, repeating the experiment with a new random reflectivity, and extracting the deconvolved spectrum as shown in Figure 18 we can see that the results are inconsistent. Figure 18 is an example of a spectrum which will yield very inaccurate AVF inversion results. This is due to the drop in amplitude at roughly 125 Hz in Figure 18, the AVF inversion scheme will see this as being caused by a negative Q value. In any case, the workflow of stacking and deconvolution followed by mean amplitude matching and then finally estimating the spectrum before inverting was performed for a number of experiments. In one of these numerical experiments the separation distance and noise level were kept constant and the target Q was varied. In another, model Q and noise level were kept constant but the separation distance was varied and finally an experiment where the separation distance and model Q were maintained constant and the noise level was varied. For each individual experiment, the inversion was performed 9 times. Table 1, 2 and 3 show the results. In table 1, the model Q ranged from 50 to 5 and for each value of Q the test was performed 9 times. Recorded in the tables is the median inversion value, the highest inversion value and the minimum inversion value. In Table 2, the model Q and the noise level were maintained constant and the separation distance was varied and in Table 3 we varied the noise level. Table 1, 2, and 3 show that AVF inversion appears to give inconsistent results especially

for small separation distances, high noise levels, and high model Q values. As model Q is lowered, we obtain more consistent results but there are still some erroneous results. For example, in Table 1 for model Q of 5 there was an anomalous inversion result of -10. The same inconsistent results holds true for the experiments where separation distance and the noise level were varied. Even at large separation distances and low noise levels there are still some anomalous inversion results.

CONCLUSION

AVF inversion provides a frequency by frequency method of inverting for anelastic parameters of a target from seismic reflection data, for example see Innanen (2011). It requires as input an estimate of the local spectrum of the absorptive reflection coefficient. In this paper, we explored practical issues affecting the implementation of AVF inversion in the presence of random noise and multiple reflection events. It was shown that proximal events interfere with the low frequency portion of the absorptive reflection and progressively affects higher frequencies as the events become more proximal. Also, an unexpected inconsistency of the AVF inversion in the presence of numerous events was observed. Namely, that there is not a systematic decrease in the fidelity of the inversion with proximity of neighboring reflections. This inconsistent result is a point of future work. The effect of a source wavelet and deconvolution on AVF inversion was also studied. It was shown that deconvolution and then mean amplitude matching between the deconvolved result and the input trace can yield inconsistent results which can lead to highly inaccurate estimates of Q. Future work will be needed to stabilize the results of AVF inversion. The authors are currently developing a least squares approach which may be useful in stabilizing AVF inversion results in the presence of a wavelet, noise and many proximal events (Bird and Innanen, 2011a).

Further, the effect of random noise was explored and it was found that random noise greatly degrades the fidelity of AVF inversion. To combat this, repeat experiments and stacking was performed and it was found that stacking helps in attenuating the random noise and improves the AVF inversion. However, in the field these repeat experiments would be costly and so stacking of CDP traces may need to be performed. Because of this, AVO effects on the spectrum of the stacked

Table 1. Inversion values for varying model Q with constant separation distance and noise level

| Actual Q | Inverted Q | Inverted Q (high) | Inverted Q (low) |
|----------|------------|-------------------|------------------|
| 50 | 9 | 53 | -74 |
| 25 | 4 | 87 | -23 |
| 15 | 10 | 93 | -70 |
| 10 | 9 | 116 | -39 |
| 7 | 9 | 24 | -9 |
| 5 | 6 | 11 | -10 |

Table 2. Inversion values for varying separation distance and constant noise level. Actual Q used in modeling is 5

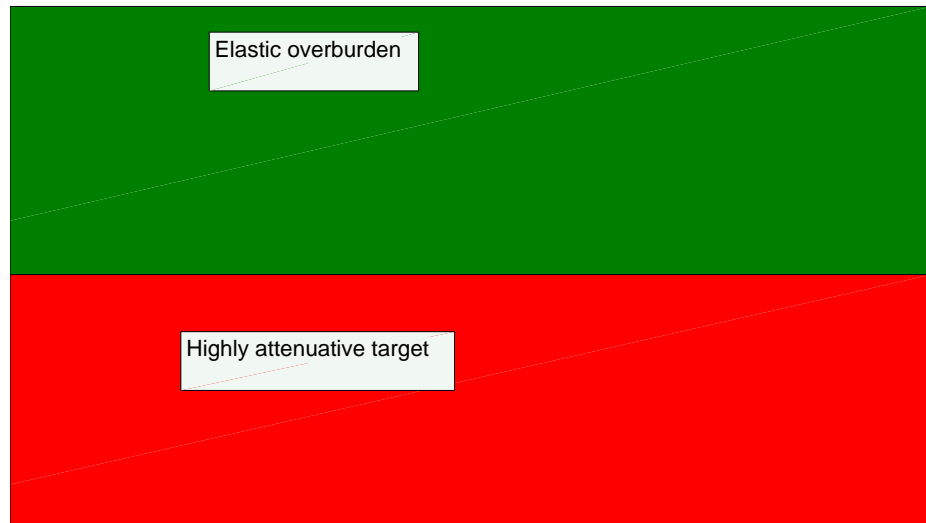


FIG. 1. In the top panel an absorptive reflection on the right and random reflectivity on the far left. Notice the large separation in time between the absorptive reflection and the other reflection events. In the bottom panel we see the FST spectrum of the absorptive reflection (red) and the FST spectrum of the absorptive reflection with the random reflectivity present (blue). Notice that the spectrum of the absorptive reflection is interfered with by the random reflectivity at low frequencies and so the low frequency information cannot be used for AVF inversion.

| separation distance | Inverted Q (median) | Inverted Q (high) | Inverted Q (low) |
|---------------------|---------------------|-------------------|------------------|
| 100 | 7 | 10 | -10 |
| 80 | 8 | 21 | -5 |
| 60 | 6 | 27 | -6 |
| 40 | 8 | 36 | -6 |
| 20 | 5 | 52 | -30 |
| 10 | 4 | 22 | -6 |

Table 3. Inversion values for varying noise level an constant separation distance. Actual Q used in modeling is 5

| noise level (%) | Inverted Q (median) | Inverted Q (high) | Inverted Q (low) |
|-----------------|---------------------|-------------------|------------------|
| 2 | 10 | 18 | -4 |
| 5 | 12 | 19 | -2 |
| 10 | 8 | 17 | -23 |

REFERENCES

- Bird, C., and Innanen, K., 2011a, Least squares avf inversion: CREWES Annual Report, **23**, 1–10.
- Bird, C., and Innanen, K., 2011b, Towards field evidence for anelastic and dispersive AVF reflections: CREWES Annual Report, **23**, 1–10.
- Bird, C., Innanen, K., Naghizadeh, M., and Lines, L., 2010a, Determination of anelastic reflectivity: how to extract seismic avf information: CREWES Annual Report, **22**, No. 4.
- Bird, C., Naghizadeh, M., and Innanen, K., 2010b, Amplitude calibration of a fast S-transform: CREWES Sponsor's Meeting 2010, **22**, 1–12.

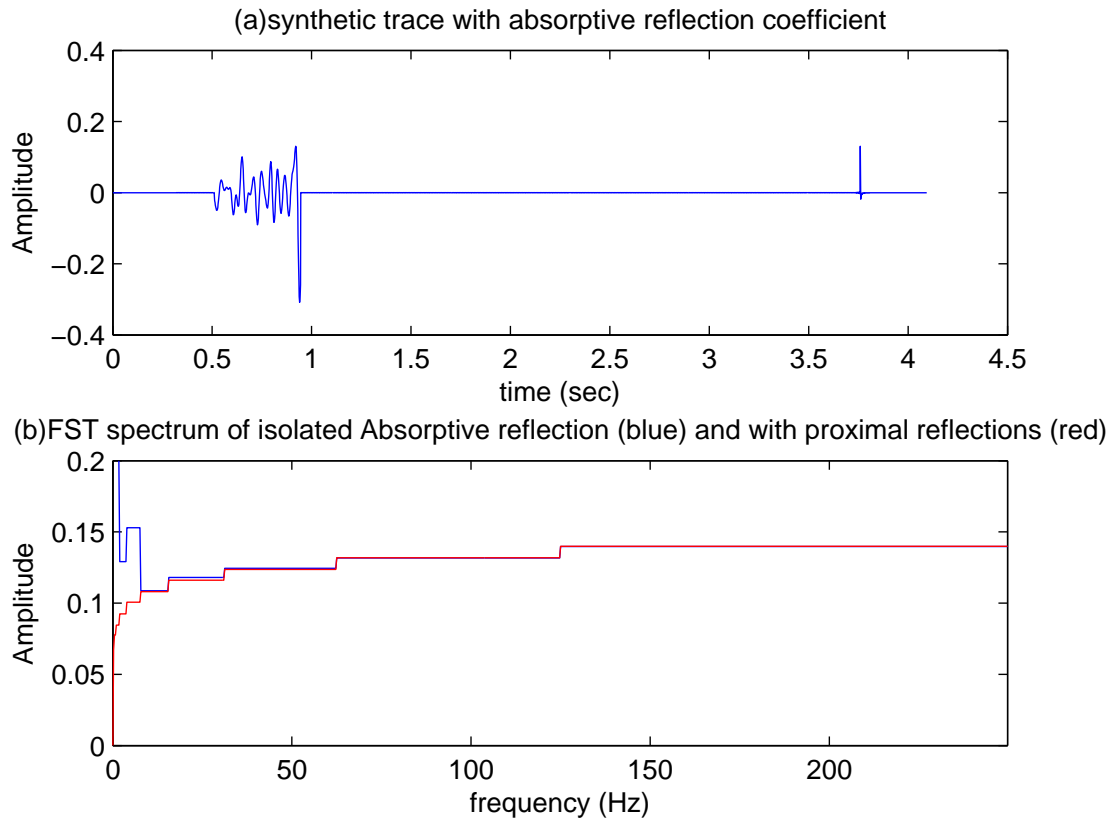


FIG. 2. In the top panel an absorptive reflection on the right and random reflectivity on the far left. Notice the large separation in time between the absorptive reflection and the other reflection events. In the bottom panel we see the FST spectrum of the absorptive reflection (red) and the FST spectrum of the absorptive reflection with the random reflectivity present (blue). Notice that the spectrum of the absorptive reflection is interfered with by the random reflectivity at low frequencies and so the low frequency information cannot be used for AVF inversion.

Innanen, K., 2011, Inversion of the seismic AVF/AVA signatures of highly attenuative targets: *Geophysics*, **76**, No. 1, R1–R14.

Lines, L., Sondergeld, C., Innanen, K., Wong, J., Treitel, S., and Ulrych, T., 2000, Experimental confirmation of "reflections on q".

Lines, L., Vasheghani, F., and Treitel, S., 2008, Reflections on Q: *CSEG Recorder*, **December**, 36–38.

Naghizadeh, M., and Innanen, K., 2010, Fast generalized Fourier interpolation of nonstationary seismic data: *CREWES Sponsor's Meeting 2010*.

Odebeatu, E., Zhang, J., Chapman, M., and Li, X.-Y., 2006, Application of spectral decomposition to detection of dispersion anomalies associated with gas saturation: *The Leading Edge*, **February**, 206–210.

O'Doherty, R. F., and Anstey, N. A., 1971, Reflections on amplitudes: *Geophysical Prospecting*, **19**, 430–458.

Quan, Y., and Harris, J. M., 1997, Seismic tomography using the frequency shift method: *Geophysics*, **62**, No. 3, 895–905.

Sheriff, R., and Geldart, L., 1995, *Exploration Seismology*: Cambridge University Press, 2nd edn.

Vasheghani, F., and Lines, L. R., 2009, Viscosity and Q in heavy-oil reservoir characterization: *The Leading Edge*, **July**, 856–860.

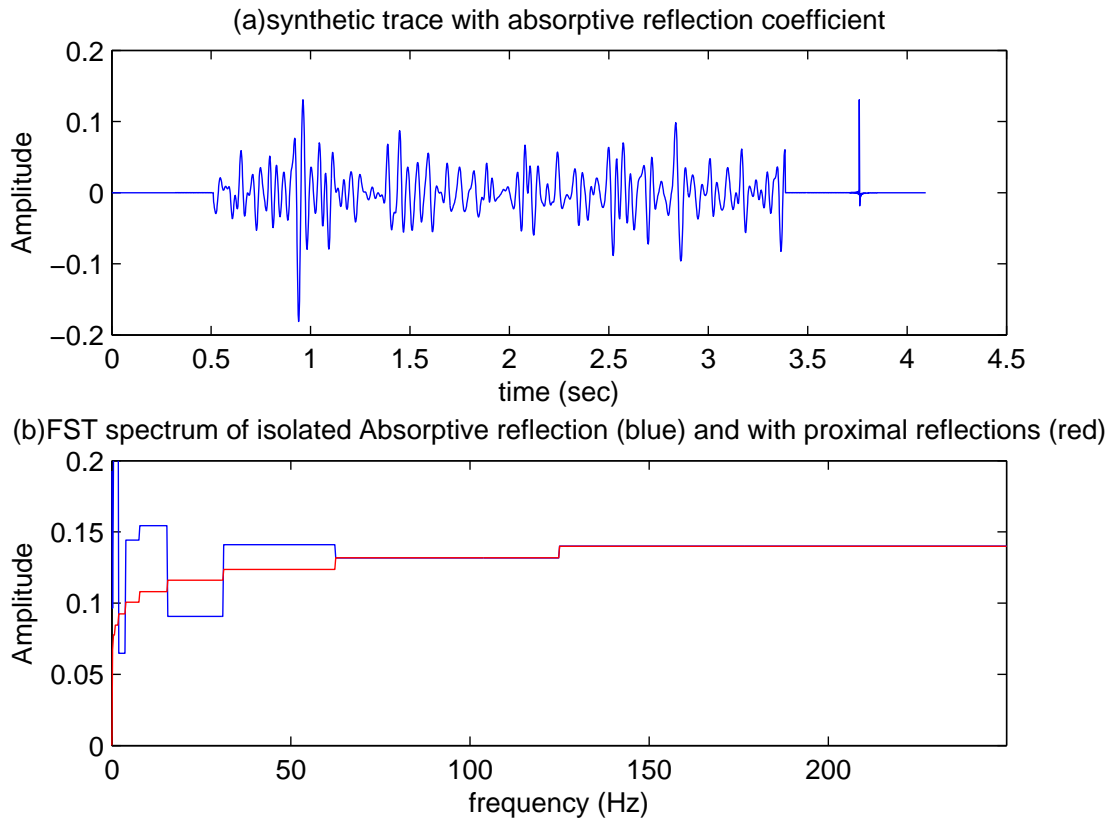


FIG. 3. In the top panel an absorptive reflection on the right and random reflectivity on the far left. Notice now that the separation in time between the absorptive reflection and the other reflection events is very small. In the bottom panel we see the FST spectrum of the absorptive reflection (red) and the FST spectrum of the absorptive reflection with the random reflectivity present (blue). Notice that the spectrum of the absorptive reflection is interfered with by the random reflectivity for a much greater bandwidth than in Figure 1. This is due to the proximity of the nearby reflectivity.

Wu, X., Chapman, M., Li, A. W., and Xi, ????, Estimating seismic dispersion from pre-stack data using frequency-dependent avo inversion.

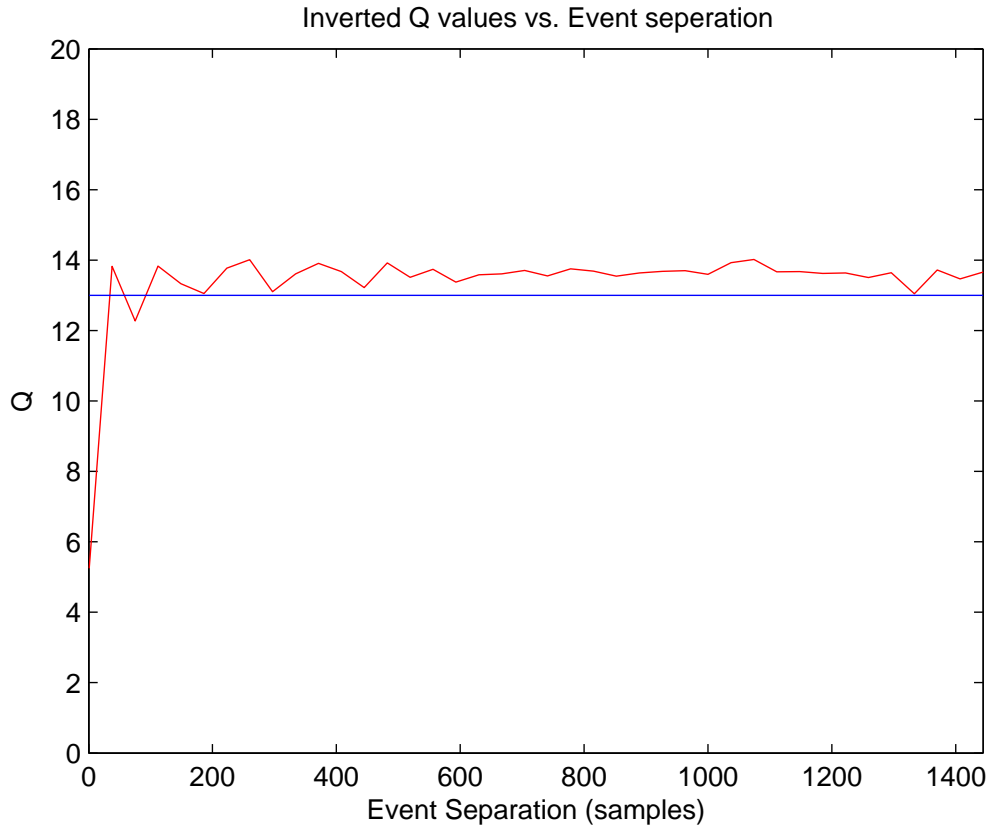


FIG. 4. AVF inversion accuracy in the presence of proximal reflection events. On the x-axis is the separation in number of samples between the absorptive reflection and the nearest event. The blue line is the actual value of Q used in the modeling and the red line is the inversion result. Notice that as the separation distance becomes very small, the inversion becomes unstable.

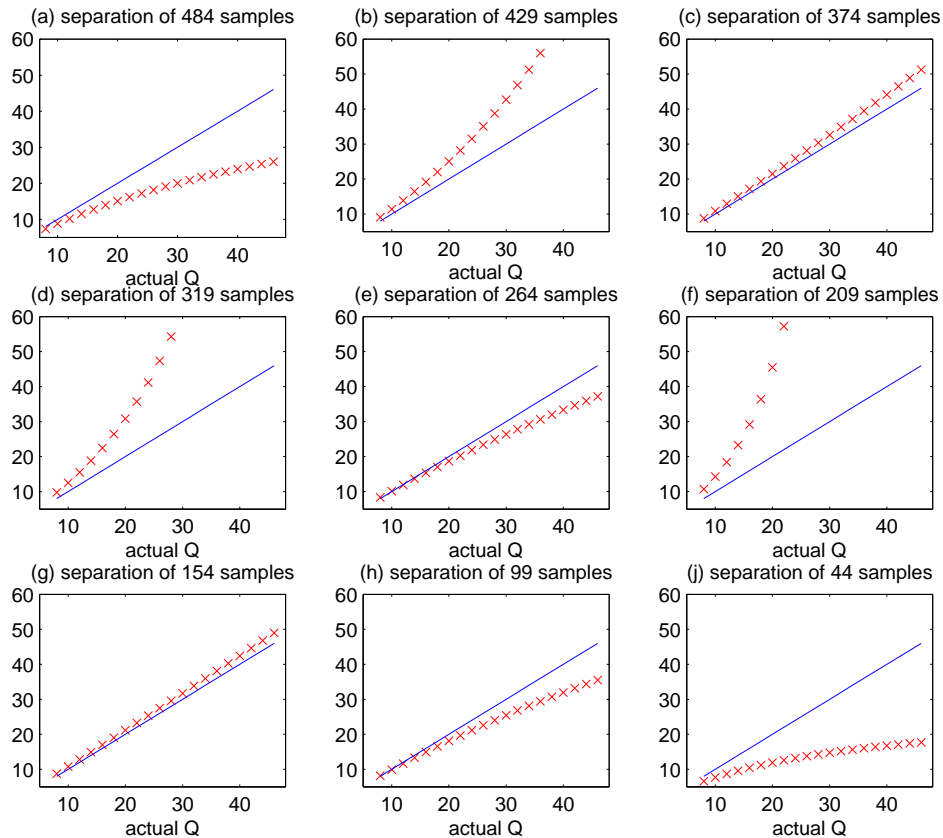


FIG. 5. 9 panels showing the accuracy of AVF inversion. Each panel is for a different separation distance. In each panel we see the inversion result (red x's) and the actual value of Q (blue). Notice that the separation distance does not appear to matter too greatly on the accuracy of the inversion. For instance, the inversion result for a separation distance of 99 samples is much better than for a separation distance of 209 samples, which is contrary to what we would expect.

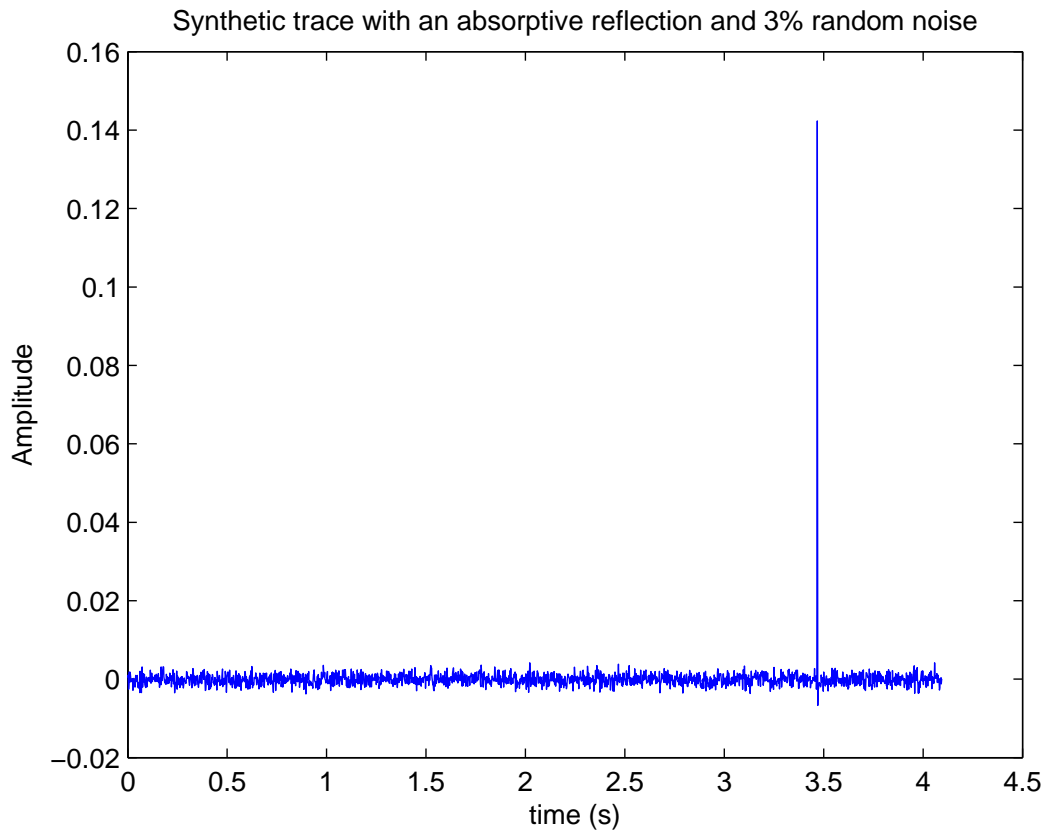


FIG. 6. A trace with a single absorptive reflection and 3% random noise.

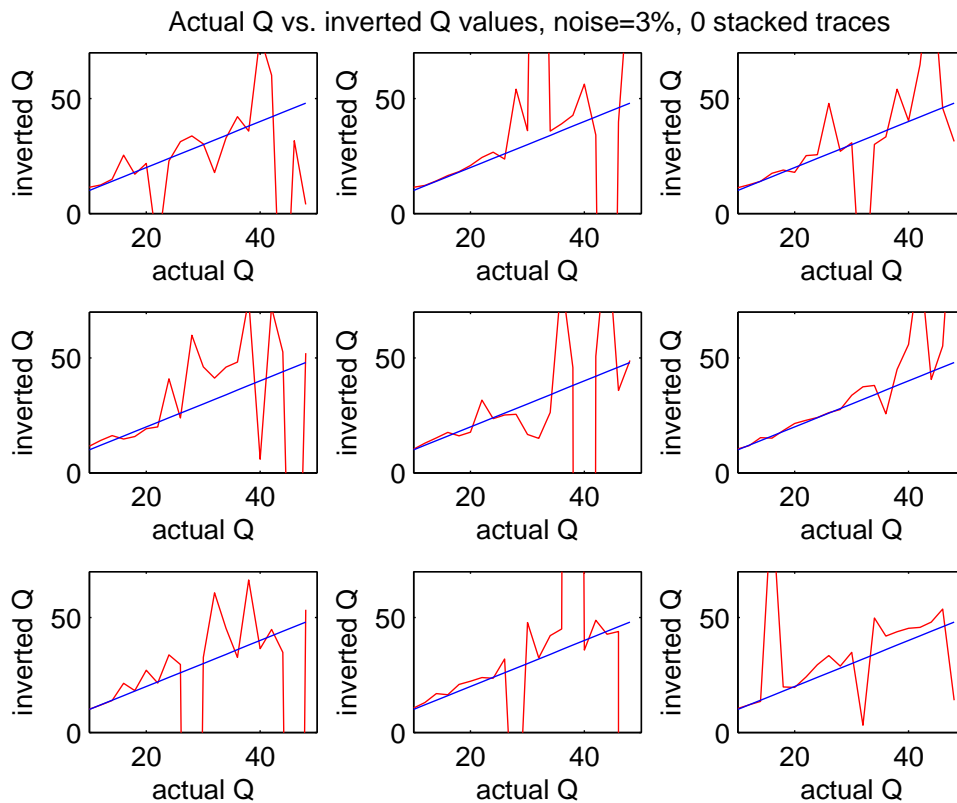


FIG. 7. Accuracy of AVF inversion in the presence of 3% random noise and no stacking. Each panel is a repeat experiment to gain statistical sampling of the inversion accuracy. Notice that the presence of noise greatly degrades the accuracy of AVF inversion.

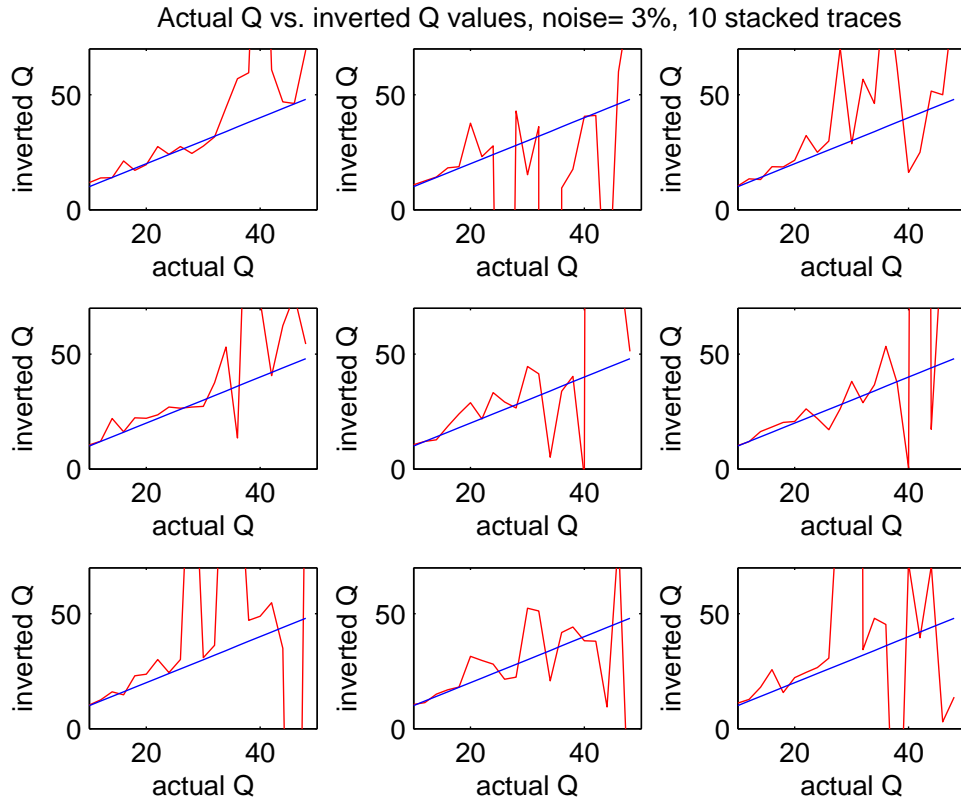


FIG. 8. Accuracy of AVF inversion in the presence of 3% random noise and 10 stacked traces. Each panel is a repeat experiment to gain statistical sampling of the inversion accuracy. Notice that stacking 10 traces has somewhat improved the accuracy of AVF inversion, especially for low Q values.

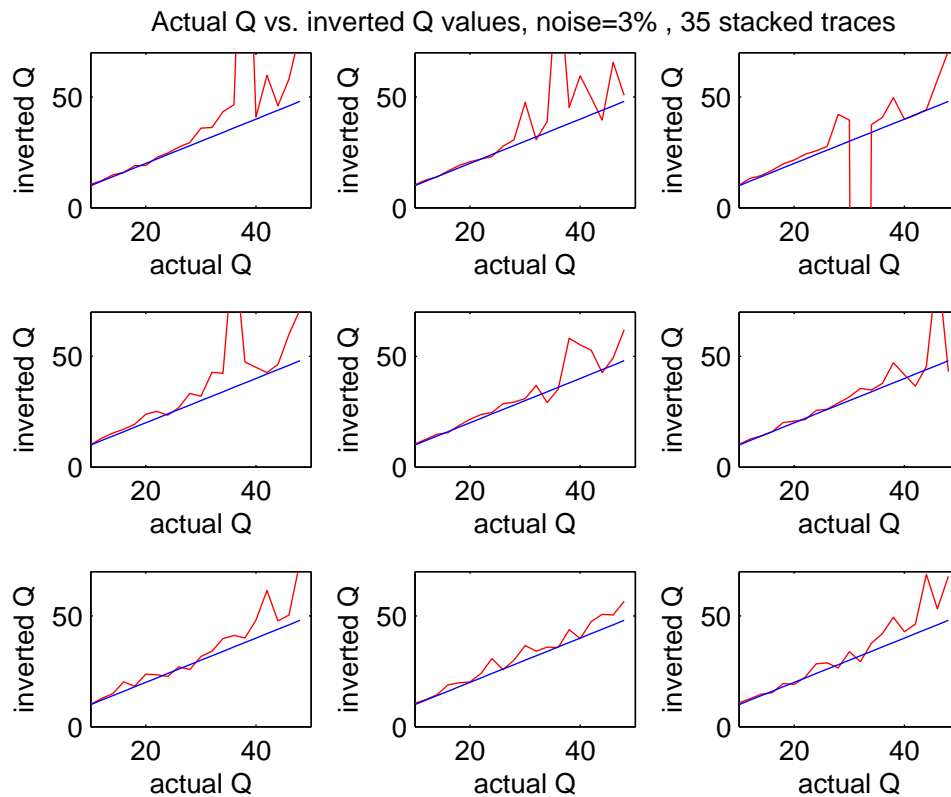


FIG. 9. Accuracy of AVF inversion in the presence of 3% random noise and 35 stacked traces. Each panel is a repeat experiment to gain statistical sampling of the inversion accuracy. Notice that stacking 35 traces has greatly improved the accuracy of AVF inversion, especially for low Q values.

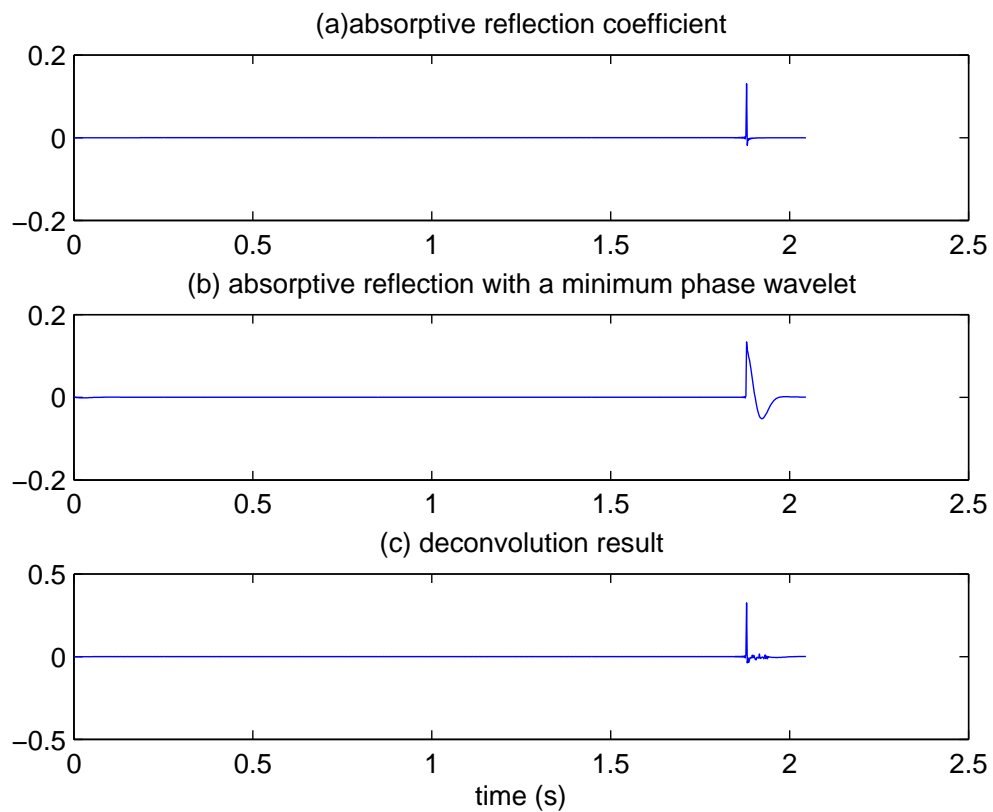


FIG. 10. In (a) an absorptive reflection coefficient. In (b) the absorptive reflection coefficient is convolved with a minimum phase wavelet and in (c) the result of deconvolving the the trace in (b) using Weiner spiking deconvolution codes from the CREWES toolbox

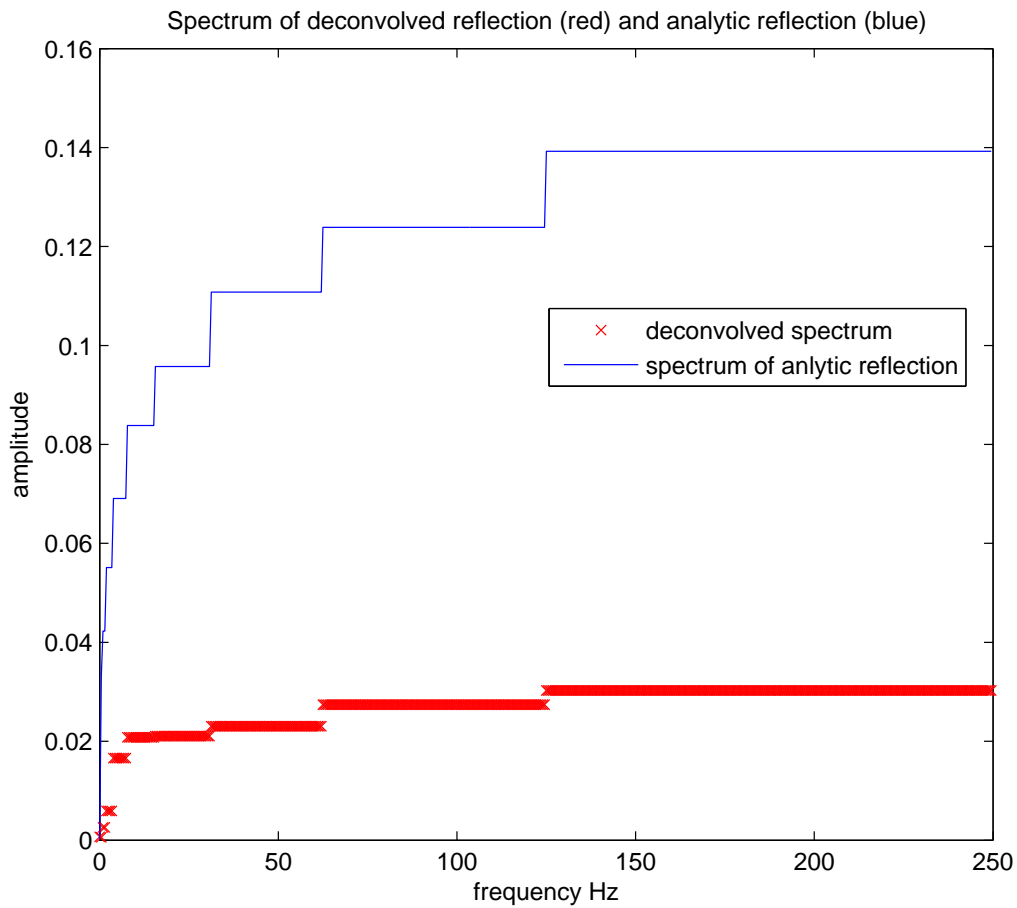


FIG. 11. The blue curve is the FST spectrum of the analytic absorptive reflection coefficient. This absorptive reflection coefficient was convolved with a minimum phase wavelet and then deconvolved using Wiener deconvolution codes and the red curve is the FST spectrum of the deconvolved result.

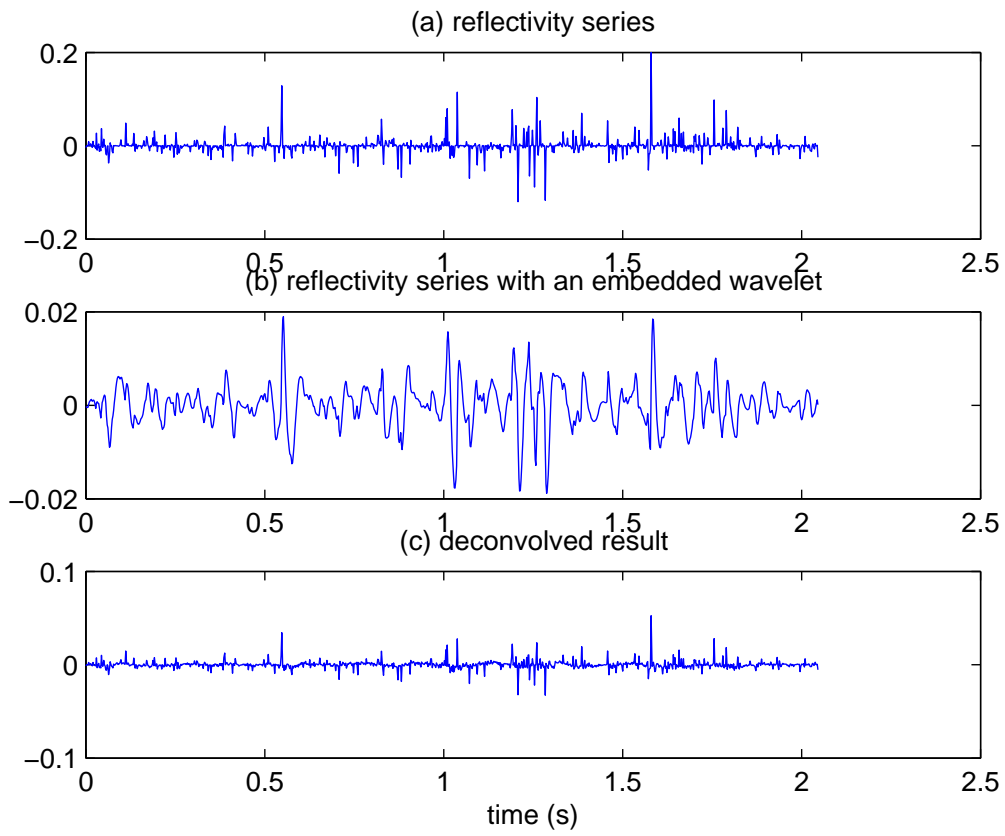


FIG. 12. In (a) a random reflectivity series. In (b) the reflectivity series is convolved with a minimum phase wavelet and (c) shows the deconvolved result

Spectrum of trace with embedded wavelet (blue) and spectrum of deconvolved result (black)

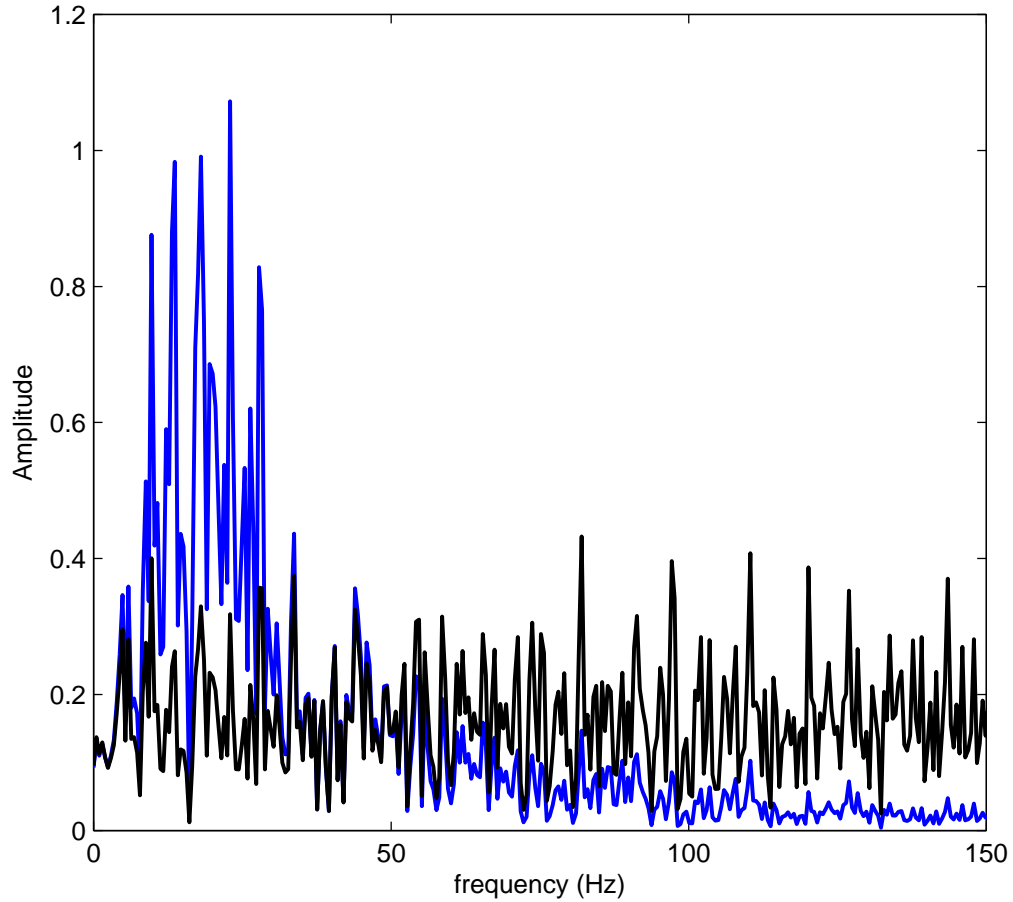


FIG. 13. The blue curve is the amplitude spectrum of a reflectivity series convolved with a wavelet. The black curve is the spectrum of the deconvolved result. RMS power matching of the deconvolution codes is performed across the entire bandwidth so the deconvolved spectrum has lower amplitudes than the original trace over the bandwidth of the source wavelet.

Spectrum of trace with embedded wavelet (blue) and spectrum of deconvolved result (black)

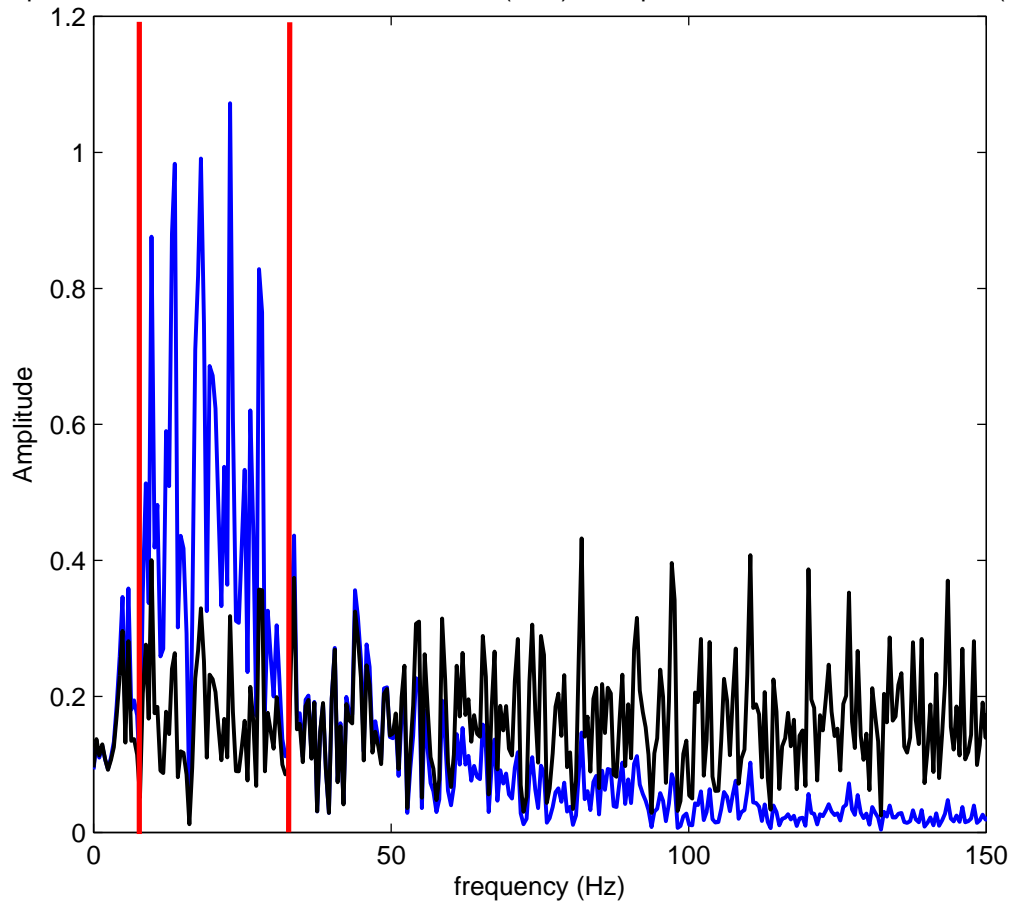


FIG. 14. The blue curve is the amplitude spectrum of a reflectivity series convolved with a wavelet. The black curve is the spectrum of the deconvolved result. RMS power matchin of the deconvolution codes is performed across the entire bandwidth so the deconvolved spectrum has lower amplitudes than the original trace over the bandwidth of the source wavelet. The vertical red lines show where the mean amplitude ratio was extracted to correct the spectrum of the deconvolved trace to implement AVF inversion.

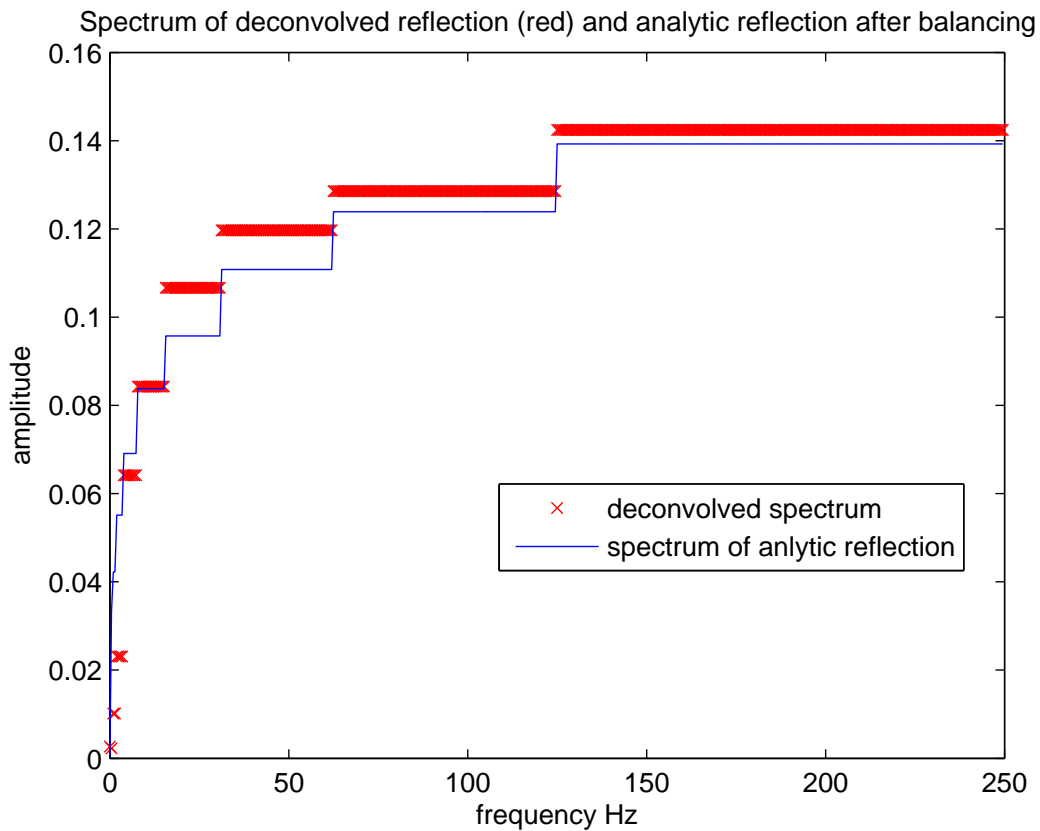


FIG. 15. The Result of mean amplitude matching the deconvolved spectrum. The blue curve is the FST spectrum of an analytic absorptive reflection coefficient. The red curve is the corrected FST spectrum of a deconvolved absorptive reflection coefficient after mean amplitude matching.

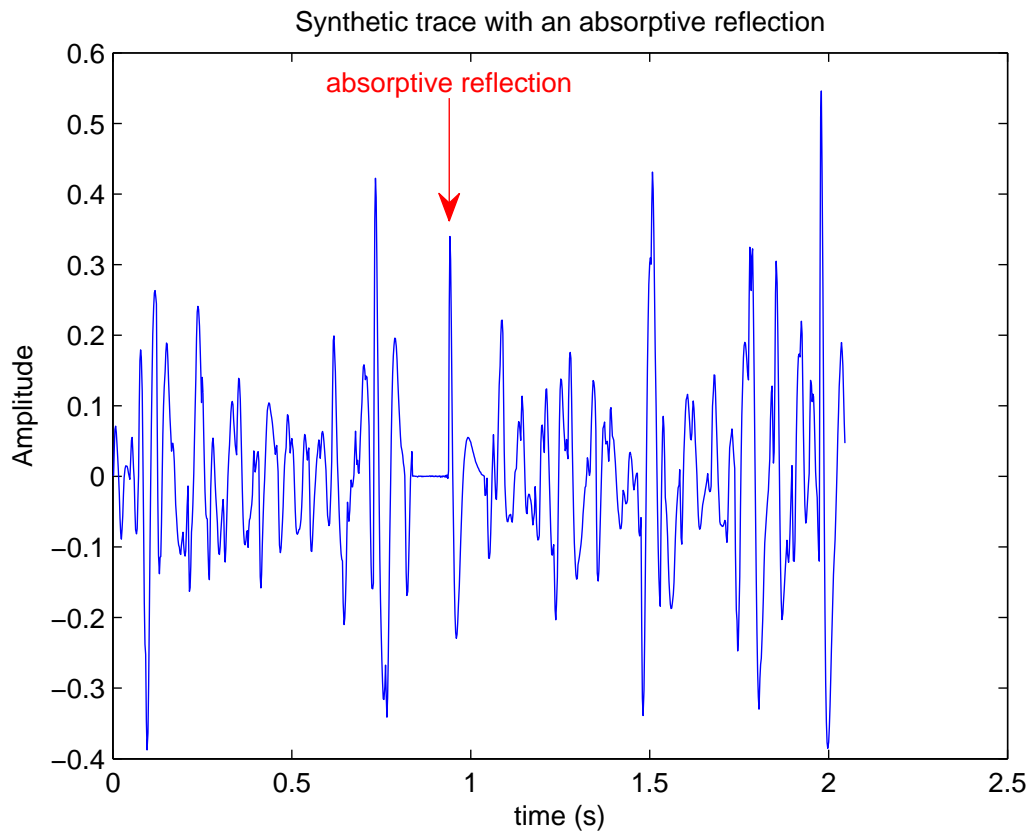


FIG. 16. A random reflectivity, with an embedded absorptive reflection coefficient, with random noise and convolved with a wavelet.

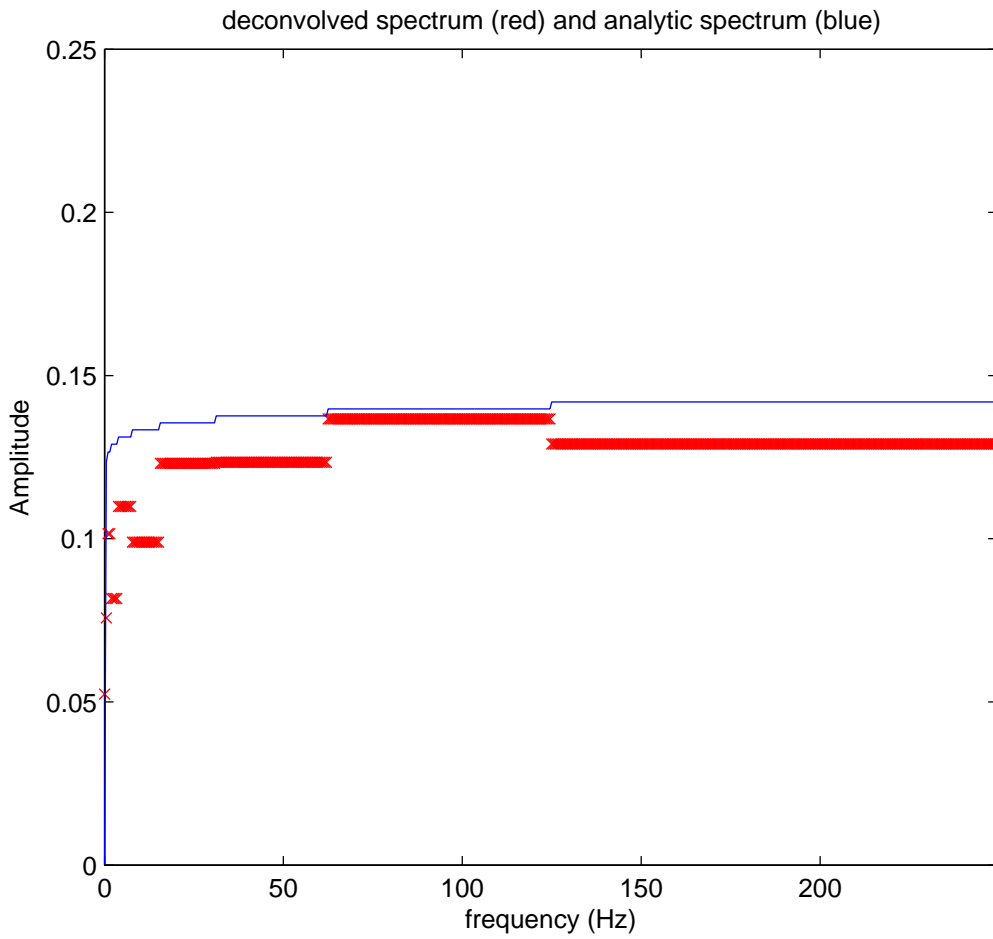


FIG. 18. The blue curve is the FST spectrum of an analytic absorptive reflection coefficient. The red curve is the corrected FST spectrum of the absorptive reflection extracted from traces shown in Figure 16